Quercetin pentaacetate inhibits *in Vitro* Human Respiratory Syncytial Virus adhesion

Bruno Rafael Pereira Lopes, Mirian Feliciano da Costa, Amanda de Genova Ribeiro, Caroline Sprendel Lima, Icaro Putinhon Caruso, Gabriela Campos de Araújo, Letícia Hiromi Kubo, Federico Iacovelli, Mattia Falconi, Alessandro Desideri, Juliana de Oliveira, Luis Octávio Regasini, Fátima Pereira Souza, Karina Alves Toledo

PII: S0168-1702(19)30353-3

DOI: https://doi.org/10.1016/j.virusres.2019.197805

Reference: VIRUS 197805

To appear in: *Virus Research*

Received Date: 27 May 2019

Revised Date: 18 October 2019

Accepted Date: 3 November 2019

Please cite this article as: Lopes BRP, da Costa MF, de Genova Ribeiro A, Lima CS, Caruso IP, de Araújo GC, Kubo LH, Iacovelli F, Falconi M, Desideri A, de Oliveira J, Regasini LO, Souza FP, Toledo KA, Quercetin pentaacetate inhibits *in Vitro* Human Respiratory Syncytial Virus adhesion, *Virus Research* (2019), doi: https://doi.org/10.1016/j.virusres.2019.197805

Quercetin pentaacetate inhibits *in Vitro* Human Respiratory Syncytial Virus adhesion

Bruno Rafael Pereira Lopes[ab], Mirian Feliciano da Costa[ab], Amanda de Genova Ribeiro[ab], Caroline Sprendel Lima[b], Icaro Putinhon Caruso[bc], Gabriela Campos de Araújo[bc], Letícia Hiromi Kubo[a], Federico Iacovelli[d], Mattia Falconi[d], Alessandro Desideri[d], Juliana de Oliveira[a], Luis Octávio Regasini[b], Fátima Pereira Souza[bc], Karina Alves Toledo[ab*]

[a]Universidade Estadual Paulista – UNESP (FCLAssis), Brazil

[b]Universidade Estadual Paulista – UNESP (IBILCE, São José do Rio Preto), Brazil

[c]Centro Multiusuário de Inovação Biomolecular (CMIB), Universidade Estadual Paulista – UNESP (IBILCE, São José do Rio Preto), Brazil

[d] Department of Biology, University of Rome Tor Vergata, Via della Ricerca Scientifica 1, 00133, Rome, Italy.

*Corresponding author: Karina Alves de Toledo, Av. Dom Antônio, 2100, Parque Universitário, CEP 19806-900, Assis/SP, Brasil. Tel: + 55-18-3302-5848; E-mail address: karina.toledo@unesp.br

HIGHLIGHTS

- Quercetin acetylation reduces its cytotoxicity on Hep-2 cells
- Quercetin acetylation improves its virucidal action on Respiratory Syncytial Virus (RSV)
- In silico data indicates interaction between Quercetin pentaacetate and F-protein is more stable than Quercetin/F-protein
- Quercetin pentaacetate interacts with RSV and inhibit the viral adhesion on cell surface

ABSTRACT

Human respiratory syncytial virus (hRSV) is one of the main etiological agents of diseases of the lower respiratory tract and is often responsible for the hospitalization of children and the elderly. To date, treatments are only palliative and there is no vaccine available. Natural products show exceptional structural diversity and they have played a vital role in drug research. Several investigations focused on applied structural modification of natural products to improved metabolic stability, solubility and biological actions them. Quercetin is a flavonoid that presents several biological activities, including anti-hRSV role. Some works criticize the pharmacological use of Quercetin because it has low solubility and low specificity. In this sense, we acetylated Quercetin structure and we used in vitro and in silico assays to compare anti-hRSV function between Quercetin (Q0) and its derivative molecule (Q1). Q1 shows lower cytotoxic

effect than Q0 on HEp-2 cells. In addition, Q1 was more efficient than Q0 to protect HEp-2 cells infected with different multiplicity of infection (0.1-1 MOI). The virucidal effects of Q0 and Q1 suggest interaction between these molecules and viral particle. Dynamic molecular results suggest that Q0 and Q1 may interact with F-protein on hRSV surface in an important region to adhesion and viral infection. Q1 interaction with F-protein showed ΔG= -14.22 kcal/mol and it was more stable than Q0. Additional, MTT and plate assays confirmed that virucidal Q1 effects occurs during adhesion step of cycle hRSV replication. In conclusion, acetylation improves anti-hRSV Quercetin effects because Quercetin pentaacetate could interact with F-protein with lower binding energy and better stability to block viral adhesion. These results show alternative anti-hRSV strategy and contribute to drug discovery and development.

Keywords: antiviral, flavonoids, respiratory virus, in silico, in vitro, HEp-2 cells

1. Introduction

The human Respiratory Syncytial Virus (hRSV) is the main cause of **a**cute **l**ower **r**espiratory **t**ract **i**nfections (ALRTI) in newborns and children, and is considered a public health issue at a global level, due to death and hospitalization rates as well as high treatment costs associated with it. hRSV infections affect approximately 70% of newborns during their first year of life and 95% of children up to 2 years, resulting in more than 3 million hospitalizations and about 200,000 deaths per year (Noor and Krilov, 2018).

The existing approaches and medicines for the treatment and management of hRSV infections such as Ribavirin and Palivizumab come with challenges like the difficulty in administration, the high cost involved in prophylaxis, as well as the generation of drug escape mutants. Thus, research into new compounds and/or the design of new strategies against hRSV is essential to reduce infection and to control its spread, especially in areas with large flow of susceptible individuals, such as hospitals, kindergartens and primary schools. The major focus of most studies is to find molecules able to inhibit hRSV surface glycoproteins G and F, whereas these proteins are responsible for the initial steps of adhesion and fusion of the virus to the host cell, and the latter is essential to guarantee the virus entry (Battles and McLellan, 2019).

A number of flavonoids like apigenin, daidzein, dinatin, luteolin, sulfuretin, naringenin, catechin, amentoflavone, baicalin, baicalein, gallocatechin, myricetin, wogonin, and isovitexin (Xiao, 2017) exhibit antiviral activity and, in particular, quercetin has demonstrated capability for inhibition of rhinovirus replication both *in vivo* and *in vitro*, antiviral effect upon HIV reverse transcriptase and other retroviruses, herpes simplex type 1, poliovirus type-1, parainfluenza type-3 and Hepatitis – C (Ganesan et al., 2012; Gonzalez et al., 2009; Kaul et al., 1985; Rojas et al., 2016;

Wu et al., 2015; Zandi et al., 2011). Nevertheless, irrespective of the aforementioned antiviral activity, solubility and stability of quercetin may be impaired in the lipophilic media of a membrane due to the presence of the OH groups. In this regard, studies have shown that the liposolubility of quercetin, especially its acetylation favors its solubility reducing its cytotoxic effect on Hela cells and increasing its anti-inflammatory capacity on an *in vivo* model (Danihelová et al., 2013, 2012; Gusdinar et al., 2011).

The aim of our study was to evaluate the impact of the chemical modification of Quercetin molecule to Quercetin pentaacetate (QPA) upon its anti-RSV activity. We also sought to pursue the interaction mechanism model of Quercetin and Q1 with hRSV-F protein through the use of classical molecular dynamics (MD) simulation.

2. Materials and methods

2.1.Reagents

Quercetin (2-(3,4-dihydroxyphenyl)-3,5,7-trihydroxychromen-4-one) was purchased from Sigma-Aldrich (St. Louis, MO, USA). Quercetin acetylation was performed as previous described (Guimarães et al., 2018). Two molecules were diluted in dimethyl sulfoxide (DMSO, Sigma-Aldrich). The stock was protected from light and maintained at -80 °C for up to one month.

2.2.Cell culture

The human laryngeal carcinoma cell line (HEp-2; Cell Bank of Rio de Janeiro, Rio de Janeiro, RJ, Brazil) was grown at 37°C, 5% CO_2 in DMEM-F12 (Sigma-Aldrich) supplemented with 10% fetal bovine serum (FBS; Cultilab, Campinas, SP, Brazil) and complemented with antibiotics and antimycotics (Invitrogen, Carlsbad, CA, USA). HEp-2 cells are derived from human respiratory tract epithelia and are permissive to hRSV infection and replication (Gupta et al., 1996).

2.3.Viral stock

Human respiratory syncytial virus (RSV) strain Long was provided by Dr. Eurico de Arruda Neto (USP, Brazil) and amplified in HEp-2 cells. The viral titer was determined via plaque reduction assay (McKimm-Breschkin, 2004) and confirmed via 50% tissue culture infective dose ($TCID_{50}$) (Rasmussen et al., 2010). Viral fractions were kept at -80 °C.

2.4.Cytotoxicity

Cytotoxicity was evaluated via MTT assay (3-(4,5-dimethylthiazol-2-yl)2,5-diphenyltetrazolium bromide, Sigma-Aldrich). HEp-2 cells (5×10^4/well) received the compound diluted in DMEM-F12 (phenol red free) with 2% FBS. After 3 days of incubation, the MTT solution was added and the absorbance was measured spectrophotometrically in a plate reader (FC™ Microplate Multiskan Photometer, Thermo Fisher Scientific Inc., Waltham, MA, USA) at 560 nm. Cells cultured in medium alone were considered 100% viable. The CC_{50} values (50% cytotoxic concentration) were determined by fitting a four-parameter nonlinear sigmoidal regression curve using GraphPad Prism 6 software (GraphPad Software, Inc., San Diego, CA, USA).

2.5.Antiviral activity

Antiviral activity was evaluated by observing cell viability and plaque formation. The viability of HEp-2 cell monolayer was evaluated by colorimetric MTT assays, using pre-treatment, virucidal and post-treatment protocols (supplementary material). In all assays, HEp-2 cells (5×10^4/well) were seeded in 96-well plates and divided in different groups: (i) hRSV infected and untreated cells were used as negative control (0% protection), (ii) untreated/non-infected cells were considered positive control (100% protection), and (iii) treated/infected cells as sample tests. The salt MTT was added to culture after incubation for 3 days at 37 ºC and 5% CO_2. The antiviral activity (% cell protection) for each treatment was calculated using the Equation 1 (supplementary material).

For plaque assay, we performed the method previously described (McKimm-Breschkin, 2004). HEp-2 cells monolayer grown in 24 well plates ($3x10^5$/well), was treated and infected according to adsorption, internalization and time-addition protocols (supplementary material). In brief, HEp-2 cells were infected with hRSV MOI 0.5 and tested compounds were added before, during and after infection (until 48hs). The culture was maintained for six days when cells were formalized and the hRSV plaques formation was evidencing by addition of 0.05% of Neutral Red (N4638, Sigma-Aldrich). The counting plaques was helped by the use a negatoscope.

2.6.Statistical analysis

Analysis of variance (ANOVA) and Kruskal-Wallis were performed using GraphPad 6 software. $p < 0.05$ was considered significant.

2.7.Molecular Modeling of the hRSV-F Glycoprotein

The Protein Data Bank (PDB) contains more than 20 crystal structures of hRSV-F Glycoprotein in complex with antibodies or inhibitors. These structures lack the three helices forming the coiled-coil in the C-terminal region and most of the mucin-like regions. To obtain the complete protein structure, we performed a modeling procedure by

submitting the corresponding sequence of hRSV-F Glycoprotein (UniProtKB: P03420, residues 1–574) to the I-TASSER web server and assigning the PDB crystal structure (ID: 4JHW) as a template. The I-TASSER server combines threading and *ab-initio* procedures and has been evaluated as the best threading modeling program in recent community-wide Critical Assessment of protein Structure Prediction (CASP) experiments (Yang et al., 2014), providing an on-line workbench for high-resolution modeling of protein structures and functions (http://zhanglab.ccmb.med.umich.edu/I-TASSER/). I-TASSER generates five models with different C-scores and structures. A C-score represents a confidence score for estimating the quality of models predicted by I-TASSER, and is calculated based on the significance of threading template alignments and the convergence parameters of the structure assembly simulations. The C-score is typically in the range of -5 to 2 and a higher value signifies a 3D model with a high confidence and vice versa (Yang et al., 2014). All 3D models produced by I-TASSER resemble the 4JHW crystal structure, and the highest C-score (equal to 0.08) was chosen to perform the final modeling. The modeled structure was then imported to UCSF Chimera (Pettersen et al., 2004), triplicated, and superimposed through the MatchMaker tool on the biological assembly of 4JHW structure to obtain the final model.

2.8.Model Preparation for Classical Molecular Dynamics Simulations

The system topology and coordinates used as input for the GPU-enabled version of *pmemd*, the MD engine included in the AMBER-12 package, were obtained through the Leap module of AmberTools12 (Case et al., 2014), assigning parameters for structures through AMBER-FF14SB force-field (Maier et al., 2015). Q0 and Q1 parameters were derived through single-point calculations performed in Gaussian-09 at HF-SCF/6-31G* level on the optimized structures to derive electrostatic potential and restrained electrostatic potential, while restrained electrostatic potential (RESP) partial charges were obtained from electrostatic potential using antechamber module in AMBER-12. The general AMBER force field (gaff) was used to parametrize the inhibitors using antechamber. The complexes were immersed in a rectangular box filled with TIP3P water molecules (Jorgensen et al., 1983), imposing a minimum distance between the solute and box of 14 Å. Charges were neutralized by adding Cl- counter-ions to solvated systems in favorable positions.

2.9.MD Protocol

A minimization run (5000 steps) was performed using the steepest descent algorithm, imposing harmonic constraint of 50 kcal·mol^{-1}·Å^{-2} to remove unfavorable interactions introduced by the modelling procedure. The system was gradually heated in the Canonical (NVT) ensemble from 0 to 300 K over a period of 500 ps using Langevin thermostat (Lzaguirre et al., 2001) with a coupling coefficient of 1.0 ps and a weak constraint of 15 kcal·mol^{-1}·Å^{-2}. In

the last equilibration step, the system was subjected to an equilibrium simulation for 1 ns, removing all constraints. The optimized system was then simulated using the isobaric-isothermal (NPT) ensemble for 20 ns, using periodic boundary conditions, a 2.0 fs time-step, a cut-off of 9.0 Å for evaluation of short-range non-bonded interactions, and the PME method for long-range electrostatic interactions. SHAKE algorithm was used to constrain covalent bonds involving hydrogen atoms. Temperature was fixed at 300 K using Langevin dynamics, while pressure was held constant at 1 atm through the Langevin piston method. The atomic positions were saved every 500 steps (1.0 ps) for analyses. The simulations were entirely performed using 2 NVIDIA TESLA C2075 GPUs.

2.10.Trajectories Analysis

The distance and hydrogen bonds between protein and ligands were evaluated using *g_dist* and *g_hbond* modules of the GROMACS 4.6.7 MD package (Hess et al., 2014). Contacts were evaluated through a home-made tool based on the python pmx package, considering all protein atoms interacting with ligands in a 4.0 Å radius. Interaction energies were evaluated through the MM-PBSA (Molecular Mechanics-Poisson-Boltzmann Surface Area) module of the Amber12 package using the MM-GBSA approach (Weiser et al., 1999). The g_cluster module of GROMACS, has been used to perform a clustering analysis using the gromos (Daura, X.; Gademann, K.; Jaun, B.; Seebach, D.; Van Gunsteren, W. F.; Mark, A. E. Peptide Folding: When Simulation Meets Experiment. Angew. Chem. Int. Ed 1999, 38 (1–2), 38: 236-240) algorithm on all the saved configurations. Structural images were obtained using VMD (Humphrey et al., 1996) and UCSF Chimera programs (Pettersen et al., 2004) while plots were obtained through the Grace plotting tool (http://plasma-gate.weizmann.ac.il/Grace/).

2.11.Molecular Docking

Protein-ligand docking was executed with the Auto-Dock/Vina 1.1.2 program, using the AutoDock/Vina PyMol plugin (Oleg Trott and Olson, 2009). Quercetin, Quercetin pentaacetate and JNJ-2408068 SDF files, downloaded from the PubChem compound database, were converted into PDB files and filled with hydrogens using the Open-Babel program (O'Boyle et al., 2011). The program SYBYL 6.0 was used to minimize the structures of compounds (Illapakurthy et al., 2003). Docking runs were performed using the protein centroid clusters as receptors obtained via clustering a previously performed molecular dynamics trajectory. Docking simulation was performed using the genetic algorithm with local gradient optimization. For each docking simulation, a box of 75x75x75 (grid points in XYZ axes) was centered over the binding site corresponding to empty cavities generated by the Phe488 residues. The affinity of docked compounds was expressed as binding energy (kcal/mol). Each docking simulation run took approximately 10 min on a dedicated Intel-i7 CPU workstation.

3. Results and discussion

The hRSV is the major cause of lower respiratory tract infection (LRTI). To date, there is no vaccine currently available and the previous approaches shows limited applicability and insufficient immunoprotection (Noor and Krilov, 2018). A large number of natural products have antiviral properties for many types of viruses (Xiao, 2017). Among them, high quercetin concentrations (≥ 100 μM) was able to inhibit 80-100% of hRSV in vitro infection/replication (Kaul et al., 1985). Previous works suggest that natural products properties can be altered by chemical modifications, such as changes in radical positions and/or addition of new radicals can enhance and/or add new biological properties (Yao et al., 2017). Here, we compared the anti-hRSV effects between Quercetin (Q0) and Quercetin pentaacetate (Q1).

Determination of CC50 for Q1 and Q0 on Hep-2 cells culture

First, we determinate Q0 and Q1 cytotoxicity concentrations for HEp-2 cells because they are hRSV permissive cells (Gupta et al., 1996). To determine the cytotoxicity concentration 50% (CC_{50}) of Quercetin and Quercetin pentaacetate we selected a range of concentrations (0.5-1,024 μM) based on previous studies (Lenard, 1996; Spehner et al., 1997; Zhang et al., 2005). HEp-2 cells were incubated with different Q0 and Q1 concentrations for 3 days and their viability was verified by MTT assay. Absorbance showed by cells incubated with medium alone was considered as 100% viability (Fig.1A). The obtained CC_{50} values for Q0 and Q1 found were 11 and 37 μM, respectively and they were determined by fitting a 4PL curve (Fig. 1A). The Quercetin pentaacetate shows lower cytotoxicity when compared with commercial Quercetin.

Q1 shows virucidal effect on hRSV infection

The anti-RSV activity of compounds was evaluated by post-treatment and virucidal protocol, using three different MOI (0.1, 0.5 and 1.0). In post-treatment, cells received the respective compound (Q0 or Q1) after hRSV infection. Q0 showed a total lack of protective effect on HEp-2 monolayer in any tested conditions under post-treatment protocol (green dots in white zone, protection < 50%, Fig.1B). Interestingly, Q1 shows relevant cell protection in post-treatment (2.5-10 μM) at lowest tested MOI (yellow dots in blue zone, protection ≥ 50%, Fig 1B). Next, we tested Q0 and Q1 in a virucidal protocol using the same previous conditions (1.2-10 μM, MOI 0.1, 0.5 and 1.0) for post-treatment. In the virucidal protocol, Q0 showed some protection at MOI 0.1 (~30% at 10 μM), but still have no relevant effect on hRSV replication (Fig.1B). The others Q0 concentrations had no effect in any MOI tested. Surprisingly, the Q1 showed great anti-hRSV virucidal effect, with relevant protection in all tested MOI's (yellow dots on blue zone, Fig 1B). At

MOI 0.1 the protection on HEp-2 cells viability at 10 μM is about 90-95%. This set of assays were repeated and microscopic observed (10x objective). The cellular control (HEp-2 hRSV-) has homogeneous monolayer, no cell detachment and no modified morphology (Fig 2). The progression of hRSV infection in untreated cells was clearly visible at 3 dpi (days post infection) by the presence of syncytium formation and cell detachment. Quercetin treated HEp-2 monolayer did not show reduction on syncytia formation in any tested condition and their overall visual appearance are similar of viral control (Fig 2, Q0 Vir). Quercetin pentaacetate treated cells showed dose dependent reduction of syncytia formation and no cell detachment in post-treatment at MOI 0.1 (Fig 2, Q1 Pos), and great reduction of syncytia formation in virucidal assay at MOI 0.1 and 0.5 (Fig 2, Q1 Vir). Indeed, at MOI 0.1 in virucidal protocol, the syncytia formation was rare and/or undetectable in bright field microscopy and overall monolayer appearance of Quercetin pentaacetate treated cells was the same of the cellular control (Fig 2, Q1 Vir MOI 0.1). The syncytia formation assay confirms the protection assay, Quercetin has low or any anti-hRSV effect in all tested conditions and Quercetin pentaacetate shows relevant anti-hRSV effect, mainly in the virucidal protocol.

Our results agree with others where low quercetin concentrations (<10 μM) did not show significant anti-hRSV (Kaul et al., 1985). The acetylation of Quercetin molecule reduced its cytotoxicity effects on HEp-2 cells and increased its anti-hRSV effect. Lin et al (1999) also observed reduced cytotoxicity on different cell lines when two biflavonoids, rhusflavanone and succedaneaflavananone, were acetylated (Lin et al., 1999). About the cytotoxicity, it could be related to Q1 be more hydrophobic than Q0. Thus, Q1 would penetrate into cells where it is protected by degradation of extracellular space. In addition, Q1 would protect the cells because its antioxidant activities (Chen et al., 2001). Quercetin itself shows cellular protective activity during Influenza virus infection (Kumar et al., 2005, 2003). The antiviral mechanisms of Quercetin are diverse and include direct interaction on virus surface and inhibition of genome replication, translation, assembly and antigen secretion. These activities were described for Hepatitis B and C and Influenza A virus infection (Cheng et al., 2015; Rojas et al., 2016; Wu et al., 2015). Derivatives from Quercetin also showed antiviral effects. Quercetin-7-glucoside inhibits Influenza A virus RNA polymerase (Gansukh et al., 2016). Quercetin 3-β-O-glucoside and Quercetin 3-rhamnoside target early steps of Ebola virus entry and Influenza A virus, respectively (Choi et al., 2009b; Qiu et al., 2016). Finally, Quercetin 7-rhamnoside interfere with Porcine Epidemic Diarrhea virus replication (Choi et al., 2009a).

Q1 interacts with F protein from hRSV in silico analysis

Both Quercetin and Quercetin pentaacetate were more efficient when they were tested in a virucidal protocol. This suggests that they may interact with hRSV surface proteins, among which hRSV fusion protein (hRSV-F). hRSV-F is essential for the fusion of the viral membrane with the host-cell plasma membrane, which initiates the infection. F-protein has been implicated also in viral attachment since RSV variants lacking both G and SH grow well in cell culture

(Karron et al., 1997; Techaarpornkul et al., 2001). Like G, the F-protein has been demonstrated to interact with immobilized heparin or cellular heparan sulfate, promoting attachment to and infection of immortalized cells (Feldman et al., 2000). F-protein is folding as trimeric molecule, prefusion, which contains fusion peptides inside its central cavity. The prefusion conformation is unstable and unable to promote infection. Thus, it refolds displacing the fusion peptides from the central cavity towards external F-protein surface. This F-protein conformation transition from prefusion to postfusion improves the contact between viral and cellular membrane (Battles and McLellan, 2019). Therefore, the inhibition of hRSV-F conformational transition is essential to obstruct the infection process.

Thus, we decided to investigate the interaction of Quercetin with hRSV-F modeled in this study (RSVmF) by docking and MD simulations (Fig. 3A). Subsequently, we verified the effect of Quercetin pentaacetate (Q1) on the stability of the hRSVmF-Q1 complex. The ligand JNJ-2408068 and the hRSVmF-JNJ-2408068 complex were used as reference-control. All the ligands (Fig. 3B) were allocated within the central cavity of hRSVmF as previous described (Battles et al., 2016), which suggested the stabilization of hRSV-F prefusion conformation by restricting the movement of that central cavity. The docking experiments indicated that Quercetin, Q1 and the reference-ligand completely fill hRSVmF central cavity and present similar interaction energies (around -6.5 kcal/mol).

In order to overcome docking limitations and further explore the conformational panorama sampled by the ligands each of the three best complexes was simulated through MD for a total time of 20 ns. The analyses of trajectories illustrate the molecules' behavior in a time-dependent evolution of distance between the center of mass of the ligand and the center of mass of the central cavity. From Figure 3C (or Supplementary videos 1-3), we can observe that Quercetin revealed an escaping trend from hRSVmF central cavity, which did not occur with the reference-ligand. On the other hand, the acetylated version of Quercetin (Q1) presented a closer interaction with the cavity when compared to Quercetin and towards the end of the trajectory showed a quite similar behavior to the reference-ligand.

The analysis of the hydrogen bonds indicates that Quercetin established only one hydrogen bond with the protein, while the reference-ligand was able to establish three different hydrogen bonds, one of which was maintained for more than 73% of the simulation time (**Table 1**). No hydrogen bonds were observed between Q1 and hRSVmF cavity residues, indicating the occurrence of hydrophobic interactions.

Table 1. Residues contact of hRSVmF in complex with Quercetin/inhibitor JNJ-2408068 along a trajectory of 20 ns.

Protein Residue	**Ligand**	**Persistence**
ASP489 CHAIN B	QRC	54.15
GLU487 CHAIN A	JNJ-2408068/R170591	41.95
ASP486 CHAIN A	JNJ-2408068/R170591	73.29

LYS498 CHAIN B	JNJ-2408068/R170591	29.43

Additional answers were obtained by MM-GBSA calculations, which allows us to estimate the contributions in energetic terms to the protein-ligand interaction. For the hRSVmF-Quercetin complex, the electrostatic interactions (EEL) stood out (-32.0 kcal/mol), although there were minor contributions of Van der Waals (VdW) (-18.2 kcal/mol). However, the hRSVmF-Q1 complex revealed an opposite tendency with higher VdW contributions (-36.0 kcal/mol) and lower EEL contributions (-21.1 kcal/mol). The ligand JNJ-2408068 presented a balance between these two types of interaction (-38.8 kcal/mol VdW and -37.9 kcal/mol EEL). By comparing the terms ΔGsolv and ΔGgas it can be inferred that Quercetin has a slightly higher affinity for the solvent than Q1. The evaluation of the term Δtotal reveals the total Gibbs free energy obtained for the formation of the hRSVmF-Quercetin, hRSVmF-Q1 and hRSVmF-JNJ-2408068 complexes. The Gibbs free energy represents a measure of how favorable the formation of a complex can be. The lower the value, the more favorable formation of the complex is. The results indicated that the interaction energy of hRSVmF-Quercetin was -4.9 Kcal/mol, that of hRSVmF-Q1 was -14.2 kcal/mol, and that of hRSVmF-reference-ligand was -22.8 kcal/mol.

The outcomes obtained by MM-GBSA calculations agree with the results of distance calculations (Fig. 3D) and the investigation of hydrogen bonds. Quercetin presented an escaping trend from the cavity, confirmed by the distance calculation and its interaction energy of -4.9 Kcal/mol. The withdrawal tendency of Q1 and the inhibitor were, however, less pronounced, as attested by distance analysis and their interaction energy of -14.2 kcal/mol and -22.8 kcal/mol, respectively. The hydrogen bonds evaluation showed that Quercetin formed a hydrogen bond and the reference-ligand three, although this type of interaction was not identified for Q1. Still, even if Q1 presented lower electrostatic contributions, and did not establish any hydrogen bonds with hRSVmF cavity residues, the interaction energy of the acetylated molecule is higher than that observed for the Quercetin reflecting the structural differences between the two molecules.

The chemical modification from Quercetin molecule to Quercetin pentaacetate implies changes in the degree of hydrophobicity and in the aromatic ring reactivity, as well as an increase in torsion and flexibility, and in a difference in the hydrogen-bonding pattern. Therefore, the replacement of the hydroxyl group for acetyl results in greater affinity for the cavity hRSVmF, although not by means of hydrogen bonds.

The simulation of the interaction of Quercetin with hRSV-F explains its virucidal effect in inoculum superior to MOI 0.1. Although the molecule may be able to interact with this protein, the interaction is weak in thermodynamic terms. It also revealed that the molecule has a tendency to escape from hRSV-F central cavity, which would not

effectively inhibit its conformational change. On the other hand, the acetylation of the molecule increases its virucidal activity, favoring the interaction with the protein cavity due to its hydrophobic features. The comparison between Q1 and JNJ-2408068 can be amplified. In vitro, JNJ-2408068 is more efficient and less cytotoxic than Q1 compound, since it is able to inhibit the RSV infection of Hep-2 cells with an CC50 > 100μM and EC50 = 0.16μM (Bonfanti et al., 2007; Sudo et al., 2005). In vivo and using inhalation strategies, JNJ-2408068 shows EC50 = 0.16 nM against RSV-A Long, which is roughly 100,000 fold more potent that the activity of ribavirin (15mM) (Andries et al., 2003), an approved compound to human use since 1986. At moment, we have not evidences about the efficiency of Q1 during in vivo infections but we know that its EC50 shows similar range (micromolar concentrations) to ribavirin.

In silico assays suggest a possible mechanism of direct Q1 anti-hRSV effect because they describe Q1 interaction on critical hRSV-F protein region for the transition from pre- to post-fusion state. The pre-fusion state of hRV-F is not able to carry out the infection and viral spread, consequently the transition pre/post-fusion conformation is crucial for viral entry and syncytia formation (Battles and McLellan, 2019). In addition, the impairing of post-fusion transition may increase the expression of hRSV-F in pre-fusion state on cell surface and improve the host immune response against hRSV (McLellan et al., 2013). In the future, biophysical, biochemical and biological assays will may evaluate the interactions between Q1 and other RSV proteins and to determine their contribution in the antiviral Q1 effects on RSV infection.

Q1 inhibits the adhesion of hRSV on Hep-2 cells

The hRSV cycle includes adsorption, internalization, transcription, translation, folding and release steps. Previous works shows that hRSV infection cycle is complete about 24-48 hpi (Huong et al., 2016; Rameix-Welti et al., 2014). Considering our results, that Q1 inhibits hRSV infection because it directly interacts with the virus, we performed specific protocols to evaluate in what steps Q1 shows its antiviral role.

First, we analyzed Q1 role during adsorption step. For this purpose, hRSV (MOI 0.5) and Q1 (1.2-10 μM) were previously incubated and added on HEp-2 monolayer at 4° C for adhesion. In this scenario, the virion adsorbs but not internalizes due to loss of membrane fluidity. Non-adsorbed particles are washed out and the cell viability evaluated by MTT 3 dpi. Cell viability from cells incubated with Q1 treated-virus was superior to 50% (yellow dots in blue zone, Fig. 4). This data indicates that Q1 was able to interacts with hRSV and it inhibited virus adsorption on cell surface. If Q1 directly interacts with the hRSV, it could also interfere with the internalization step. To verify this possibility, precooled HEp-2 cells were incubated with hRSV (MOI 0.5) at 4 °C for 2 h. The cell monolayer was washed and the virus internalization was permitted during 2 h at 37 °C in the presence of different Q1 concentrations. After this period, the supernatant was removed to wash the cells with citrate buffer (8.4 g of citric acid, 0.75 g of KCl and 8 g of NaCl in 1 L – pH = 3,0) and then with medium (Muller et al., 2012). After three days, the MTT assays revelated any effect of Q1 on hRSV internalization (yellow dots in white zone, Fig. 4). Finally, we evaluated Q1 effects during intracellular

steps of hRSV infection cycle. For this, HEp-2 cells were incubated with Q1 (6μM) during (0h) and after (3-48h) hRSV (MOI 0.5) infection. One more time, Q1 protected cells from viral infection during the first stages of infection cycle (yellow dots in blue zone, fig. 4; 0h). The protector effect was reduced (<50%) during the next hours (3-24 h) when hRSV is using cellular machinery to transcript, to translate and to fold in those times (Huong et al., 2016; Rameix-Welti et al., 2014). At 36 hpi, Q1 came back to show anti-hRSV effect. In this time, the new hRSV particles were released from cells, and are targeted by Q1 again. Similar results were obtained when 3 and 12μM Q1 was tested (data not shown). To confirm Q1 effects during the first stages of hRSV cycle we performed the adhesion protocol using plaque reduction assay. The plaque reduction assay is considered a "gold standard" in virology due their specificity, sensitivity and capability to explicit visually the effect of compound under the viral replication. As expected, Q1 greatly reduced the plaque forming in HEp-2 hRSV infected monolayer in all tested concentrations (Fig. 5).

In conclusion, the acetylation of Quercetin reduced cytotoxic effects and improved its anti-hRSV properties. The pentacetilated Quercetin shows virucidal effects, because it probably hinders the hRSV F-protein conformational transition from pre- to post-fusion state, thus inhibiting the viral adsorption on cell surface.

Conflict of Interest

The authors declare that the research was conducted in the absence of commercial or financial relationships that could be construed as a potential conflict of interest.

Acknowledgments

We thank Coordenação de Aperfeiçoamento de Pessoal de Nível Superior (CAPES; master's scholarship) and Fundação de Amparo à Pesquisa do Estado de São Paulo (FAPESP; Grant 2014/12298-7) for financial assistance and UNESP for structure support.

References

Andries, K., Moeremans, M., Gevers, T., Willebrords, R., Sommen, C., Lacrampe, J., Janssens, F., Wyde, P.R., 2003. Substituted benzimidazoles with nanomolar activity against respiratory syncytial virus. Antiviral Res. https://doi.org/10.1016/j.antiviral.2003.07.004

Battles, M.B., Langedijk, J.P., Furmanova-Hollenstein, P., Chaiwatpongsakorn, S., Costello, H.M., Kwanten, L., Vranckx, L., Vink, P., Jaensch, S., Jonckers, T.H.M., Koul, A., Arnoult, E., Peeples, M.E., Roymans, D., McLellan, J.S., 2016. Molecular mechanism of respiratory syncytial virus fusion inhibitors. Nat. Chem. Biol. https://doi.org/10.1038/nchembio.1982

Battles, M.B., McLellan, J.S., 2019. Respiratory syncytial virus entry and how to block it. Nat. Rev. Microbiol. https://doi.org/10.1038/s41579-019-0149-x

Bonfanti, J.F., Doublet, F., Fortin, J., Lacrampe, J., Guillemont, J., Muller, P., Queguiner, L., Arnoult, E., Gevers, T., Janssens, P., Szel, H., Willebrords, R., Timmerman, P., Wuyts, K., Janssens, F., Sommen, C., Wigerinck, P., Andries, K., 2007. Selection of a respiratory syncytial virus fusion inhibitor clinical candidate, part 1: Improving the pharmacokinetic profile using the structure-property relationship. J. Med. Chem. https://doi.org/10.1021/jm070143x

Case, D.A., Babin, V., Berryman, J., Betz, R.M., Cai, Q., Cerutti, D.S., Cheatham Iii, T.E., Darden, T.A., Duke, R.E., Gohlke, H., 2014. Amber 14.

Chen, Y.C., Shen, S.C., Lee, W.R., Hou, W.C., Yang, L.L., Lee, T.J.F., 2001. Inhibition of nitric oxide synthase inhibitors and lipopolysaccharide induced inducible NOS and cyclooxygenase-2 gene expressions by rutin, quercetin, and quercetin pentaacetate in RAW 264.7 macrophages. J. Cell. Biochem. https://doi.org/10.1002/jcb.1184

Cheng, Z., Sun, G., Guo, W., Huang, Y., Sun, W., Zhao, F., Hu, K., 2015. Inhibition of hepatitis B virus replication by quercetin in human hepatoma cell lines. Virol. Sin. https://doi.org/10.1007/s12250-015-3584-5

Choi, H.J., Kim, J.H., Lee, C.H., Ahn, Y.J., Song, J.H., Baek, S.H., Kwon, D.H., 2009a. Antiviral activity of quercetin 7-rhamnoside against porcine epidemic diarrhea virus. Antiviral Res. https://doi.org/10.1016/j.antiviral.2008.10.002

Choi, H.J., Song, J.H., Park, K.S., Kwon, D.H., 2009b. Inhibitory effects of quercetin 3-rhamnoside on influenza A virus replication. Eur. J. Pharm. Sci. https://doi.org/10.1016/j.ejps.2009.03.002

Danihelová, M., Veverka, M., Šturdík, E., Jantová, S., 2013. Antioxidant action and cytotoxicity on HeLa and NIH-3T3 cells of new quercetin derivatives. Interdiscip. Toxicol. https://doi.org/10.2478/intox-2013-0031

Danihelová, M., Viskupičová, J., Šturdík, E., 2012. Lipophilization of flavonoids for their food, therapeutic and

cosmetic applications. Acta Chim. Slovaca. https://doi.org/10.2478/v10188-012-0010-6

Feldman, S.A., Audet, S., Beeler, J.A., 2000. The Fusion Glycoprotein of Human Respiratory Syncytial Virus Facilitates Virus Attachment and Infectivity via an Interaction with Cellular Heparan Sulfate. J. Virol. https://doi.org/10.1128/jvi.74.14.6442-6447.2000

Ganesan, S., Faris, A.N., Comstock, A.T., Wang, Q., Nanua, S., Hershenson, M.B., Sajjan, U.S., 2012. Quercetin inhibits rhinovirus replication in vitro and in vivo. Antiviral Res. https://doi.org/10.1016/j.antiviral.2012.03.005

Gansukh, E., Kazibwe, Z., Pandurangan, M., Judy, G., Kim, D.H., 2016. Probing the impact of quercetin-7-O-glucoside on influenza virus replication influence. Phytomedicine. https://doi.org/10.1016/j.phymed.2016.06.001

Gonzalez, O., Fontanes, V., Raychaudhuri, S., Loo, R., Loo, J., Arumugaswami, V., Sun, R., Dasgupta, A., French, S.W., 2009. The heat shock protein inhibitor quercetin attenuates hepatitis C virus production. Hepatology. https://doi.org/10.1002/hep.23232

Guimarães, G.C., Piva, H.R.M., Araújo, G.C., Lima, C.S., Regasini, L.O., de Melo, F.A., Fossey, M.A., Caruso, Í.P., Souza, F.P., 2018. Binding investigation between M2-1protein from hRSV and acetylated quercetin derivatives: 1H NMR, fluorescence spectroscopy, and molecular docking. Int. J. Biol. Macromol. https://doi.org/10.1016/j.ijbiomac.2017.12.141

Gupta, C.K., Leszczynski, J., Gupta, R.K., Siber, G.R., 1996. Stabilization of respiratory syncytial virus (RSV) against thermal inactivation and freeze-thaw cycles for development and control of RSV vaccines and immune globulin. Vaccine 14, 1417–1420. https://doi.org/10.1016/S0264-410X(96)00096-5

Gusdinar, T., Herowati, R., Kartasasmi, R.E., Adnyana, I.K., 2011. Anti-inflammatory and Antioxidant Activity of Quercetin-3, 3', 4'-Triacetate. J. Pharmacol. Toxicol. https://doi.org/10.3923/jpt.2011.182.188

Hess, B., Spoel, D. van der, Lindahl, E., and the GROMACS development team, 2014. Gromacs User Manual Version 4.6.7, SpringerReference. https://doi.org/10.1007/SpringerReference_28001

Humphrey, W., Dalke, A., Schulten, K., 1996. VMD: Visual molecular dynamics. J. Mol. Graph. https://doi.org/10.1016/0263-7855(96)00018-5

Huong, T.N., Iyer Ravi, L., Tan, B.H., Sugrue, R.J., 2016. Evidence for a biphasic mode of respiratory syncytial virus transmission in permissive HEp2 cell monolayers Negative-strand RNA viruses. Virol. J. https://doi.org/10.1186/s12985-016-0467-9

Illapakurthy, A.C., Sabnis, Y.A., Avery, B.A., Avery, M.A., Wyandt, C.M., 2003. Interaction of artemisinin and its related compounds with hydroxypropyl-β-cyclodextrin in solution state: Experimental and molecular-modeling studies. J. Pharm. Sci. https://doi.org/10.1002/jps.10319

Jorgensen, W.L., Chandrasekhar, J., Madura, J.D., Impey, R.W., Klein, M.L., 1983. Comparison of simple potential functions for simulating liquid water. J. Chem. Phys. https://doi.org/10.1063/1.445869

Karron, R.A., Buonagurio, D.A., Georgiu, A.F., Whitehead, S.S., Adamus, J.E., Clements-Mann, M. Lou, Harris, D.O., Randolph, V.B., Udem, S.A., Murphy, B.R., Sidhu, M., 1997. Respiratory syncytial virus (RSV) SH and G proteins are not essential for viral replication in vitro: clinical evaluation and molecular characterization of a cold-passaged. Proc. Natl. Acad. Sci. U. S. A. 94, 13961–6.

Kaul, T.N., Middleton, E., Ogra, P.L., 1985. Antiviral effect of flavonoids on human viruses. J. Med. Virol. https://doi.org/10.1002/jmv.1890150110

Kumar, P., Khanna, M., Srivastava, V., Tyagi, Y.K., Raj, H.G., Ravi, K., 2005. Effect of quercetin supplementation on lung antioxidants after experimental influenza virus infection. Exp. Lung Res. https://doi.org/10.1080/019021490927088

Kumar, P., Sharma, S., Khanna, M., Raj, H.G., 2003. Effect of quercetin on lipid peroxidation and changes in lung morphology in experimental influenza virus infection. Int. J. Exp. Pathol. https://doi.org/10.1046/j.1365-2613.2003.00344.x

Lenard, J., 1996. Negative-strand virus M and retrovirus MA proteins: All in a family? Virology. https://doi.org/10.1006/viro.1996.0064

Lin, Y.M., Flavin, M.T., Schure, R., Chen, F.C., Sidwell, R., Barnard, D.L., Huffman, J.H., Kern, E.R., 1999. Antiviral activities of biflavonoids. Planta Med. https://doi.org/10.1055/s-1999-13971

Lzaguirre, J.A., Catarello, D.P., Wozniak, J.M., Skeel, R.D., 2001. Langevin stabilization of molecular dynamics. J. Chem. Phys. https://doi.org/10.1063/1.1332996

Maier, J.A., Martinez, C., Kasavajhala, K., Wickstrom, L., Hauser, K.E., Simmerling, C., 2015. ff14SB: Improving the Accuracy of Protein Side Chain and Backbone Parameters from ff99SB. J. Chem. Theory Comput. https://doi.org/10.1021/acs.jctc.5b00255

McKimm-Breschkin, J.L., 2004. A simplified plaque assay for respiratory syncytial virus - Direct visualization of plaques without immunostaining. J. Virol. Methods. https://doi.org/10.1016/j.jviromet.2004.02.020

McLellan, J.S., Chen, M., Leung, S., Graepel, K.W., Du, X., Yang, Y., Zhou, T., Baxa, U., Yasuda, E., Beaumont, T., Kumar, A., Modjarrad, K., Zheng, Z., Zhao, M., Xia, N., Kwong, P.D., Graham, B.S., 2013. Structure of RSV fusion glycoprotein trimer bound to a prefusion-specific neutralizing antibody. Science (80-.). https://doi.org/10.1126/science.1234914

Muller, V.D.M., Russo, R.R., Oliveira Cintra, A.C., Sartim, M.A., De Melo Alves-Paiva, R., Figueiredo, L.T.M., Sampaio, S.V., Aquino, V.H., 2012. Crotoxin and phospholipases A 2 from Crotalus durissus terrificus showed antiviral activity against dengue and yellow fever viruses. Toxicon. https://doi.org/10.1016/j.toxicon.2011.05.021

Noor, A., Krilov, L.R., 2018. Respiratory syncytial virus vaccine: where are we now and what comes next? Expert Opin. Biol. Ther. https://doi.org/10.1080/14712598.2018.1544239

O'Boyle, N.M., Banck, M., James, C.A., Morley, C., Vandermeersch, T., Hutchison, G.R., 2011. Open Babel: An Open chemical toolbox. J. Cheminform. https://doi.org/10.1186/1758-2946-3-33

Oleg Trott, Olson, A.J., 2009. AutoDock Vina: Improving the Speed and Accuracy of Docking with a New Scoring Function, Efficient Optimization, and Multithreading. J. Comput. Chem. https://doi.org/10.1002/jcc

Pettersen, E.F., Goddard, T.D., Huang, C.C., Couch, G.S., Greenblatt, D.M., Meng, E.C., Ferrin, T.E., 2004. UCSF Chimera--a visualization system for exploratory research and analysis. J. Comput. Chem. https://doi.org/10.1002/jcc.20084

Qiu, X., Kroeker, A., He, S., Kozak, R., Audet, J., Mbikay, M., Chrétien, M., 2016. Prophylactic Efficacy of Quercetin 3-β- O -d-Glucoside against Ebola Virus Infection . Antimicrob. Agents Chemother. https://doi.org/10.1128/aac.00307-16

Rameix-Welti, M.A., Le Goffic, R., Hervé, P.L., Sourimant, J., Rémot, A., Riffault, S., Yu, Q., Galloux, M., Gault, E., Eléouët, J.F., 2014. Visualizing the replication of respiratory syncytial virus in cells and in living mice. Nat. Commun. https://doi.org/10.1038/ncomms6104

Rasmussen, L., Maddox, C., Moore, B.P., Severson, W., White, E.L., 2010. A High-Throughput Screening Strategy to Overcome Virus Instability. Assay Drug Dev. Technol. https://doi.org/10.1089/adt.2010.0298

Rojas, N., Del Campo, J.A., Clement, S., Lemasson, M., García-Valdecasas, M., Gil-Gómez, A., Ranchal, I., Bartosch, B., Bautista, J.D., Rosenberg, A.R., Negro, F., Romero-Gómez, M., 2016. Effect of quercetin on Hepatitis C virus life cycle: From viral to host targets. Sci. Rep. https://doi.org/10.1038/srep31777

Spehner, D., Drillien, R., Howley, P.M., 1997. The assembly of the measles virus nucleoprotein into nucleocapsid-like particles is modulated by the phosphoprotein. Virology. https://doi.org/10.1006/viro.1997.8568

Sudo, K., Miyazaki, Y., Kojima, N., Kobayashi, M., Suzuki, H., Shintani, M., Shimizu, Y., 2005. YM-53403, a unique anti-respiratory syncytial virus agent with a novel mechanism of action. Antiviral Res. https://doi.org/10.1016/j.antiviral.2004.12.002

Techaarpornkul, S., Barretto, N., Peeples, M.E., 2001. Functional Analysis of Recombinant Respiratory Syncytial Virus Deletion Mutants Lacking the Small Hydrophobic and/or Attachment Glycoprotein Gene. J. Virol. https://doi.org/10.1128/jvi.75.15.6825-6834.2001

Weiser, J., Shenkin, P.S., Still, W.C., 1999. Approximate atomic surfaces from linear combinations of pairwise overlaps (LCPO). J. Comput. Chem. https://doi.org/10.1002/(SICI)1096-987X(19990130)20:2<217::AID-JCC4>3.0.CO;2-A

Wu, W., Li, R., Li, X., He, J., Jiang, S., Liu, S., Yang, J., 2015. Quercetin as an antiviral agent inhibits influenza a virus (IAV) Entry. Viruses. https://doi.org/10.3390/v8010006

Xiao, J., 2017. Dietary flavonoid aglycones and their glycosides: Which show better biological significance? Crit. Rev.

Food Sci. Nutr. https://doi.org/10.1080/10408398.2015.1032400

Yang, J., Yan, R., Roy, A., Xu, D., Poisson, J., Zhang, Y., 2014. The I-TASSER suite: Protein structure and function prediction. Nat. Methods. https://doi.org/10.1038/nmeth.3213

Yao, H., Liu, J., Xu, S., Zhu, Z., Xu, J., 2017. The structural modification of natural products for novel drug discovery. Expert Opin. Drug Discov. https://doi.org/10.1080/17460441.2016.1272757

Zandi, K., Teoh, B.T., Sam, S.S., Wong, P.F., Mustafa, M., Abubakar, S., 2011. Antiviral activity of four types of bioflavonoid against dengue virus type-2. Virol. J. https://doi.org/10.1186/1743-422X-8-560

Zhang, W., Yang, H., Kong, X., Mohapatra, S., San Juan-Vergara, H., Hellermann, G., Behera, S., Singam, R., Lockey, R.F., Mohapatra, S.S., 2005. Inhibition of respiratory syncytial virus infection with intranasal siRNA nanoparticles targeting the viral NS1 gene. Nat. Med. https://doi.org/10.1038/nm1174

Figure captions

Fig. 1. Cytotoxicity and anti-hRSV effect of Quercetin (Q0) and Quercetin pentaacetate (Q1). HEp-2 cells monolayer were incubated with respective compound for 3 days, the viability evaluated by MTT assay at 560 nm. Cell and medium only was considered 100% viable and the CC50, 11 μM for Quercetin and 37 μM for Quercetin pentaacetate, was determined by fitting a sigmoidal 4PL curve (**A**). The anti-hRSV effect of compounds was assayed in post-treatment and virucidal protocols with three MOI's (0.1, 0.5 and 1). The protection for each condition was calculated by formula (supplementary formula X). Quercetin do not show relevant protection in all tested conditions (green dots in white zone, protection < 50%). Quercetin pentaacetate shows protection in posttreatment with MOI 0.1 and shows significant protection in all tested MOI in virucidal protocol (yellow dots in blue zone, protection >= 50%) (**B**). The graphs represent the average ± S.D. from three independents experiments performed in triplicate.

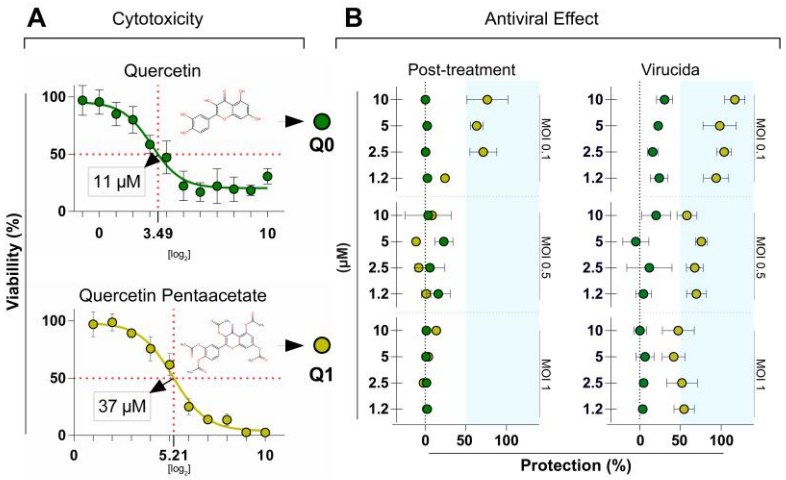

Fig. 2. Bright field microscopy aspect of hRSV syncytia formation upon HEp-2 monolayer. The progression of infection in HEp-2 monolayer (syncytia formation) in post-treatment and virucidal assays 3 dpi were analyzed and photographed in inverted microscope under 10x objective. The cellular control (HEp-2 hRSV-) shows homogeneous monolayer, no cell detachment and no syncytium formation (**A**). In infection control (HEp-2 hRSV+) the monolayer is heterogeneous, with cell detachment and syncytium formation (**B**). Quercetin treated HEp-2 cells do not reduce the syncytium formation and the monolayer aspect are similar to infection control in all tested conditions (e.g. Q0 Vir). Quercetin pentaacetate treated cells show dose dependent reduction of syncytia formation and no cell detachment in post-treatment at MOI 0.1, and great reduction of syncytia formation in virucidal assay at MOI 0.1 and 0.5 (Q1 Vir). (**C**) The summarized results (syncytium number and total area) were obtained from ImageJ software (see supplementary Fig.2. for absolute numbers)

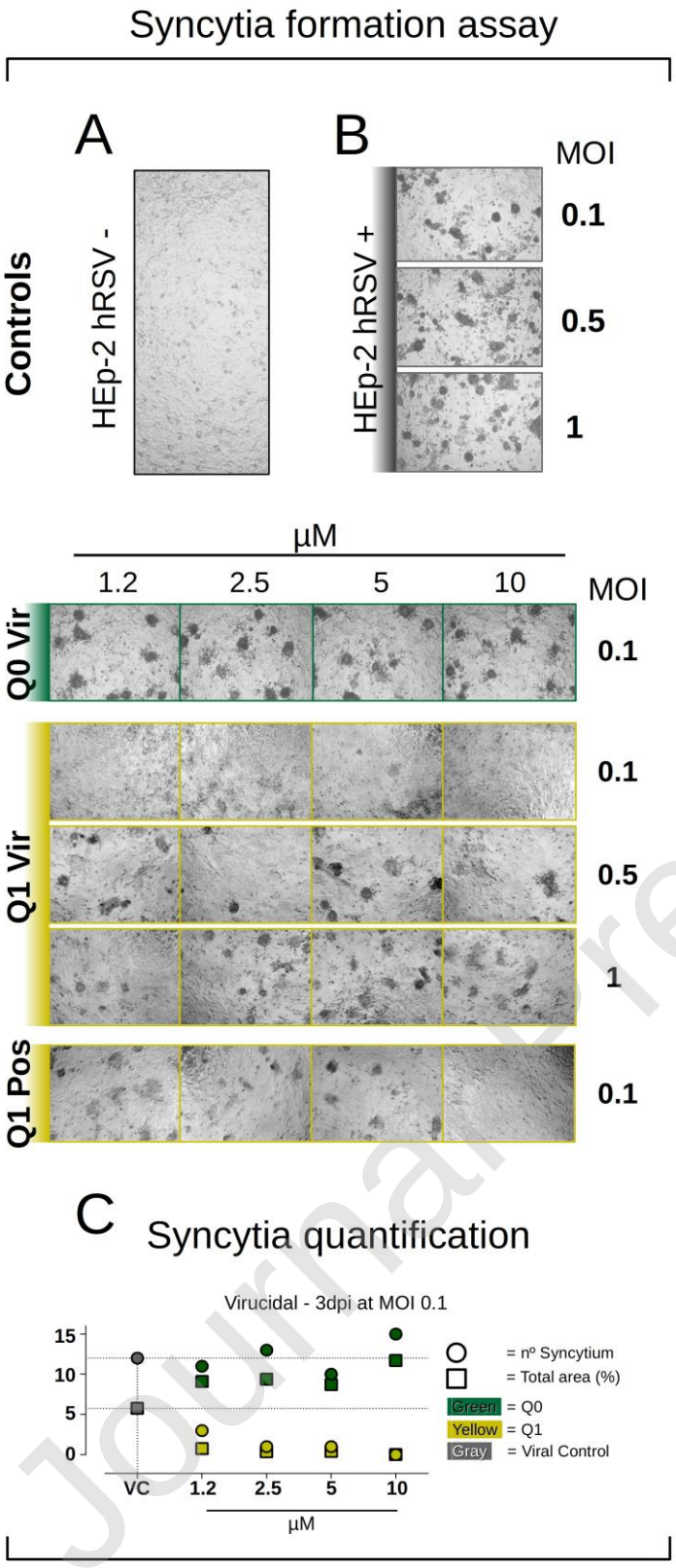

Fig. 3. hRSV-F protein model. In details, the three-fold-symmetric pocket (**A**). Small molecules assayed through molecular dynamics in complex with hRSVF (**B**). Some frames from molecular dynamics of complexes between hRSVF and small molecules. JNJ-2408068 is represented by blue color, Quercetin is green, Quercetin pentaacetate is

yellow and hRSVF pocket is white. The distance in nm from the hRSVF pocket is shown in the bottom panel (**C**). Evaluation of different energy types involved in hRSVF-small molecules interaction. Quercetin (Q0) is represented by dark green color, Quercetin pentaacetate (Q1) is light green and inhibitor JNJ-2408068 (INH) is blue. (EGB: the electrostatic contribution to the solvation free energy calculated by PB (Poisson-Boltzmann equation) or GB (Generalized Born equation); ΔG SO: EGB+ESUR; ESUR: nonpolar contribution to the solvation free energy calculated by the model; VDW: van der Walls contribution; EEL: electrostatic energy; ΔG GA free Gibbs energy from gaseous phase; ΔTotal: total energy (**D**).

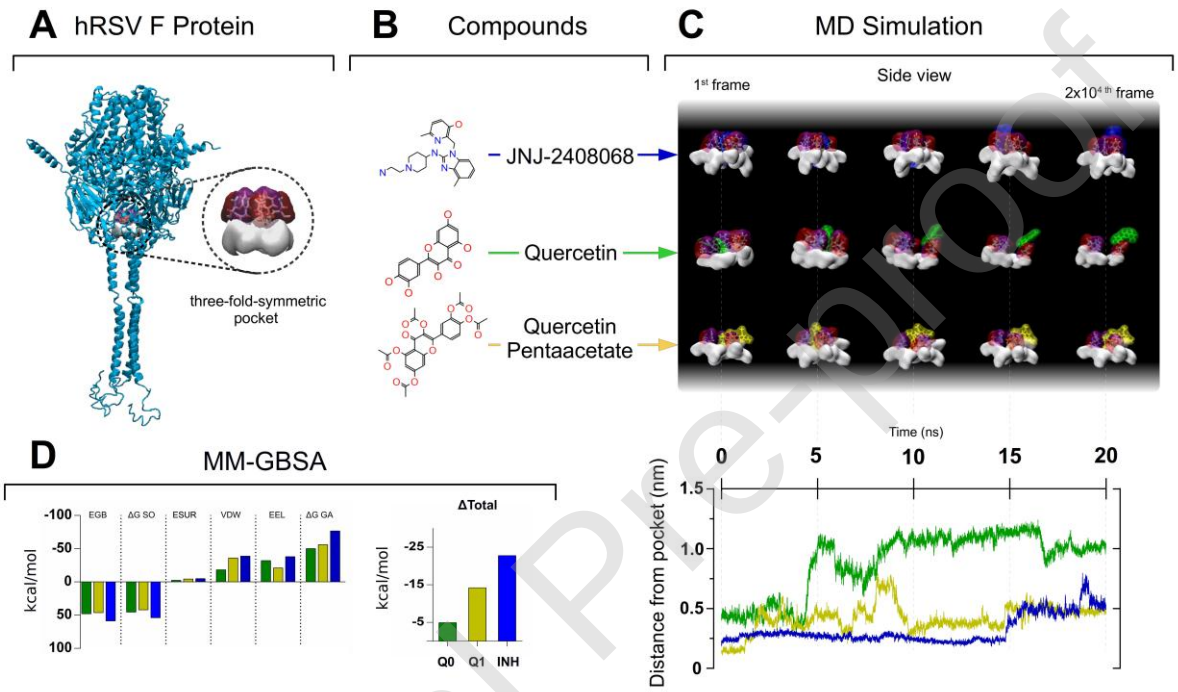

Fig. 4. Effect of Quercetin pentaacetate in hRSV cycle. The effect of Quercetin pentaacetate (Q1) in hRSV cycle was assayed in adsorption, internalization and time addition protocols with MOI 0.5 and the viability of HEp-2 monolayer was evaluated 3dpi by MTT assay at 560 nm. The protection for each condition was calculated by formula (supplementary formula X). Q1 shows great protection on adsorption assay in all tested concentrations (yellow dots on blue zone, 1.2-10 μM) at MOI 0.5. In Internalization protocol, Q1 do not show any effect on hRSV infection (yellow dots on white zone). Additionally, Q1 (6μM) only show significant protection in time addition protocol in 0 and 36 hpi. The graphs represent the average ± S.D. from three independents experiments performed in triplicate.

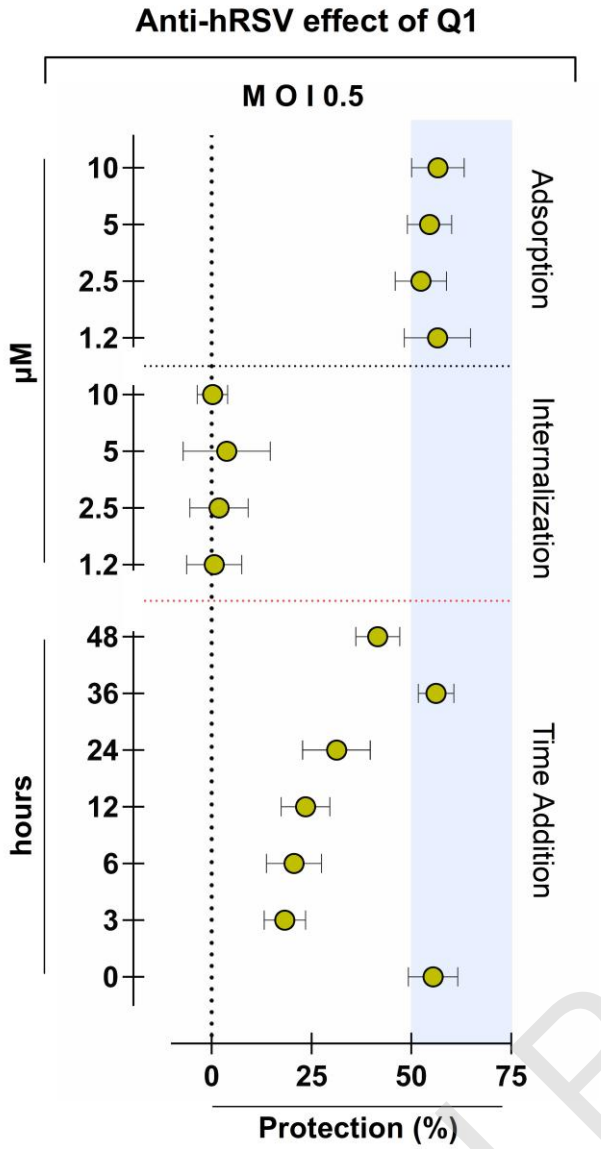

Fig. 5. hRSV plaque reduction assay of Quercetin pentaacetate (Q1) in adhesion protocol. HEp-2 cell monolayer are treated in adhesion protocol with Q1 and hRSV MOI 0.5 in 24 well plate. At 6 dpi, cell were formalized and dyed with neutral red (0.01%). The Quercetin pentaacetate reduced hRSV focus formation (black dots) in HEp-2 cells in adhesion protocol at 37 °C (1.2-10 μM) (**A**). The plates were visually counted with the aid of a negatoscope (**B**). CC = cellular control and VC = viral control.